VIP The following Communications have been judged by at least two referees to be "very important papers" and will be published online at www.angewandte.org soon:

Books

Author Profile

Correspondence

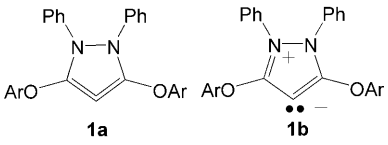

A pyrazole derivative, considered as the stable five-membered cyclic allene **1a** by Dyker, Bertrand, et al., is reinterpreted to be a zwitterion **1b**. It is shown that the bonding characteristics typical for an allene are not possible for structure **1a**. Ar = 2,6-dimethylphenyl.

Allene/Zwitterion (1)

The true ground state of **1** is a matter of debate, but for clarity and convenience the allene resonance form **1a**, is the most appropriate. The arguments for aromaticity made by Christl and Engels are shown to be incorrect.

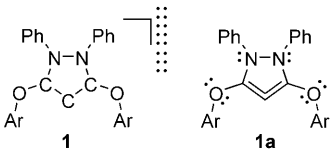

Ar = 2,6-dimethylphenyl

Allene/Zwitterion (2)

Contents

Highlights

'Onium rings: Incorporation of the trivalent oxygen atom as a structural element within the tricyclic core of **1**–**3** imparts unprecedented stability to this "extraordinary" class of tertiary oxonium ions. Cation **1** is the least reactive and can be refluxed in water for 72 hours with no noticeable decomposition.

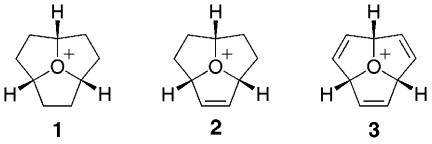

A powerful fluoride trap: The extremely Lewis acidic silyl cation $[Et_3Si]^+$ is an active catalyst for the hydrodefluorination of fluoroalkyl groups at room temperature (see example). The carborane anion $[CHB_{11}H_5Cl_6]^-$ plays an essential role in the catalytic cycle as a weakly coordinating anion that stabilizes cationic intermediates.

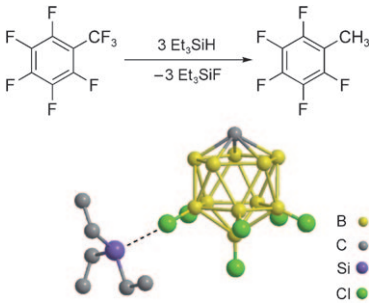

Reviews

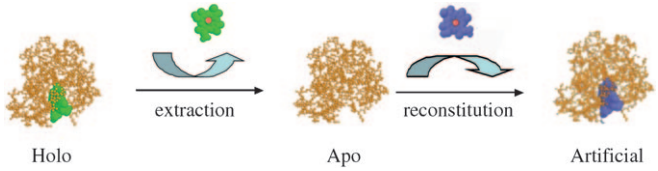

Enzymes with artificial cofactors: Non-diffusible organic cofactors of enzymes can often be replaced by artifical analogues to generate semisynthetic enzymes (see scheme). This approach can be used to study structure–function relationships in enzymology and to produce novel enzymes with enhanced or even entirely new functions that are useful for biosensing, biocatalysis, and materials science applications.

For the USA and Canada: ANGEWANDTE CHEMIE International Edition (ISSN 1433-7851) is published weekly by Wiley-VCH, PO Box 191161, 69451 Weinheim, Germany. Air freight and mailing in the USA by Publications Expediting Inc., 200 Meacham Ave., Elmont, NY 11003. Periodicals postage paid at Jamaica, NY 11431. US POSTMASTER: send address changes to *Angewandte Chemie*, Wiley-VCH, 111 River Street, Hoboken, NJ 07030. Annual subscription price for institutions: US$ 7225/6568 (valid for print and electronic / print or electronic delivery); for individuals who are personal members of a national chemical society prices are available on request. Postage and handling charges included. All prices are subject to local VAT/sales tax.

Communications

Finely tuned: A stable dye-sensitized solar cell that contains a molecularly engineered organic dye has been prepared. The efficiency of the cell remains at 90% after 1000 h of light soaking at 60°C. The remarkable stability of the cell is also reflected in the open-circuit voltage value (V_{oc}), short-circuit photocurrent-density value (J_{sc}), and the fill factor, which also show barely no decline (see picture).

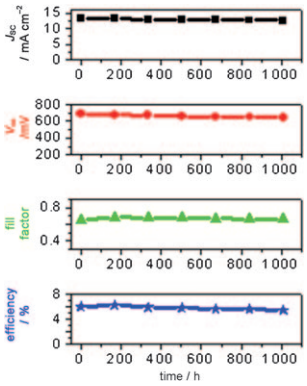

Molecular Solar Cells

Wheels of steel: Two enantiomerically pure chiral {Fe_{28}} wheel-like aggregates have been synthesized from the acetate buffer solution containing ferric ions and chiral tartrate ligands (see picture). These compounds are the largest chiral ferric aggregates isolated to date.

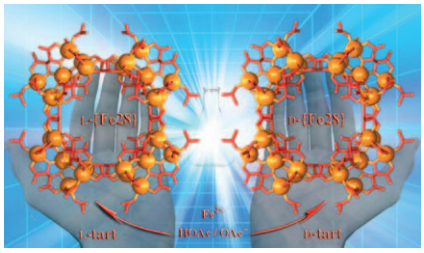

Chiral Materials

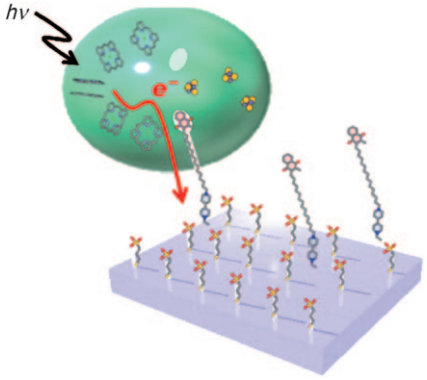

Plug and play: Photoinduced electron transfer occurs from photoexcited P700 in photosystem I (PSI) to a gold surface (see picture). A novel molecular connector system is used, in which an artificial molecular wire, which is assembled on the gold surface, was plugged into PSI by reconstitution. Analysis of the photoelectron transfer kinetics proved both the output of electrons from PSI and the effectiveness of the molecular wire.

Photoelectron Transfer

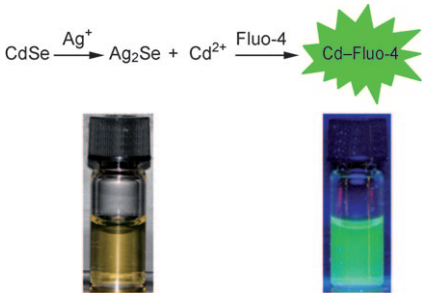

Lighting-up time: A cation-exchange reaction releases thousands of divalent cations from nonfluorescent CdSe ionic crystals and triggers fluorescence from thousands of originally nonfluorescent Fluo-4 fluorophores to obtain a large fluorescence amplification (see picture) and a low detection limit in bioassays. The technique is fast, simple, with a large dye-to-reporter labeling ratio, and flexible in selection of nanocrystals and fluorophores.

Biosensors

Incredibly swift

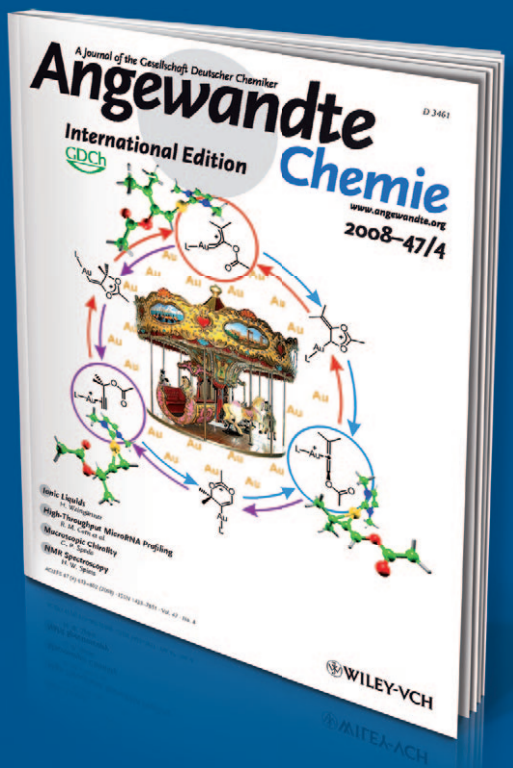

...!

Manuscripts submitted to *Angewandte Chemie* can be published in a matter of days, and that's including meticulous peer review, careful copy-editing, and author proofing. **The peer-review process requires an average of just 13 days, and 30% of all Communications are brought to readers within two months after submission of the original manuscript.** The articles are not only published rapidly, they are also swiftly assimilated within the scientific community, as reflected by the extremely high Immediacy Index of *Angewandte Chemie* (2007: 2.271).

GDCh
Gesellschaft Deutscher Chemiker

www.angewandte.org
service@wiley-vch.de

WILEY-VCH

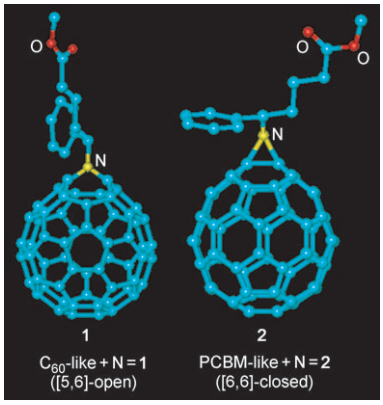

Crossing the bridge: Two isomeric iminofullerenes, [5,6]-open azafulleroid **1** and [6,6]-closed aziridinofullerene **2**, were prepared by cycloaddition of an organic azide to C_{60}. These "azalogues" enable the study of the effects of the bridging atom in a fullerene cage, that is, C_{60}-like (5,6-open) versus PCBM-like (6,6-closed), as a function of their π systems (PCBM = [6,6]-phenyl-C_{61}-butyric acid methyl ester).

Fullerenes

Molecular dynamics simulations reveal that the key factors that determine the ability of an additive to modulate crystal nucleation are the strength of its interaction with the solute, its disruptive ability (which may be based on steric, entropic, or energetic effects), and interfacial properties, along with its ability to serve as a template for nucleation (see snapshot of an emerging nucleus with a single-particle additive: black spheres).

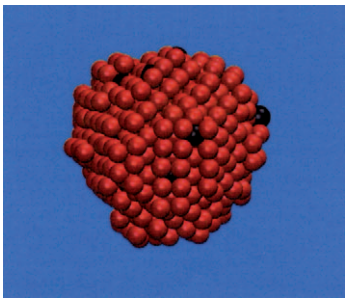

Crystal Engineering

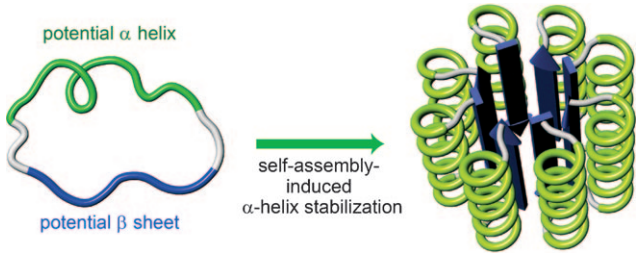

Protein roll call: Peptide-based building blocks, in which both an α-helix-forming segment and a β-sheet segment are located within a single macrocyclic structure, self-assemble into α-helix-decorated artificial proteins. This approach provides a starting point for developing artificial proteins that can modulate α-helix-mediated interactions occurring in a multivalent fashion.

Artificial Proteins

Shewanella is an electrogenic microbe that has significant content of *c* type cytochromes (ca. 0.5 mM). This feature allows the optical absorption spectra of the cell-membrane-associated proteins to be monitored in vivo in the course of extracellular respiratory electron-transfer reactions. The results show significant differences to those obtained in vitro with purified proteins.

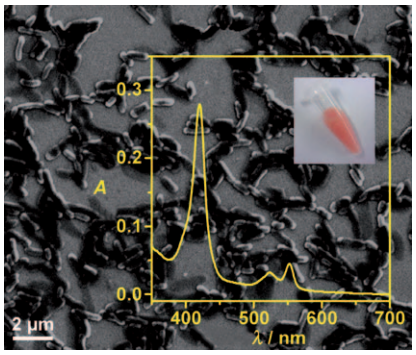

In Vivo Proteins

Contents

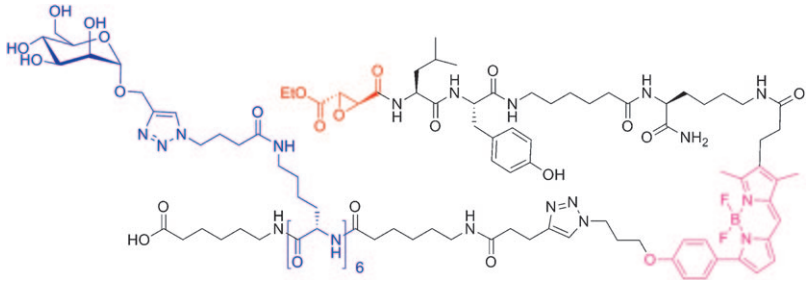

Tag for professionals: A fluorescently tagged clustered mannoside DCG-04 analogue (see structure) is designed and synthesized using a modular approach. Uptake of the probe in professional antigen presenting cells and subsequent labeling of cathepsins proceeded in a mannose-receptor dependent manner.

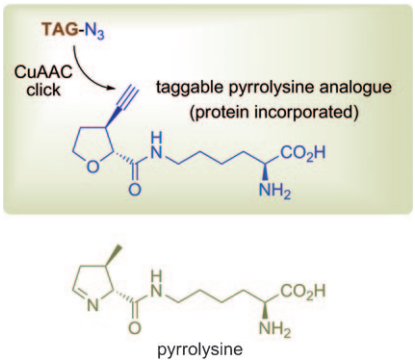

Ignoring the STOP sign: A pyrrolysine analogue bearing a terminal alkyne was site-specifically incorporated into recombinant calmodulin (CaM) through a UAG codon. The resulting protein was labeled with an azide-containing dye using a copper(I)-catalyzed click reaction. Subsequent application of an orthogonal cysteine tagging method yielded a CaM labeled with two distinct fluorophores that enabled its study by FRET spectroscopy.

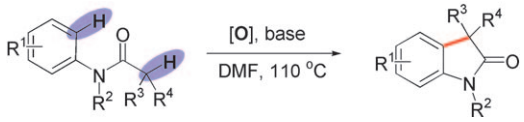

An sp^2/sp^3 get-together: A novel and efficient method can be used to synthesize 3,3-disubstitued oxindoles by the direct intramolecular oxidative coupling of an aryl C_{sp^2}–H and a C_{sp^3}–H center (see scheme; DMF = *N*,*N*-dimethylformamide).

Great bowls of fire: The rotation of the cyclopentadienyl (Cp) ring is restricted in two concave-bound monoalkyl-substituted $[CpFe(\eta^6\text{-sumanene})]^+$ "π-bowl" complexes (see picture). The asymmetric stacking of atropisomers was observed with a MeCpFe complex in the solid state and the chiral (*S*)-*s*BuCpFe complex showed magnetic and optical desymmetrization of the sumanene ligand, which is the first example of a chiral complex of a π-bowl ligand.

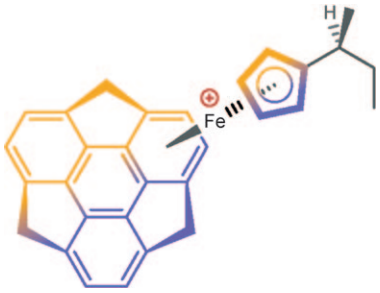

Contents

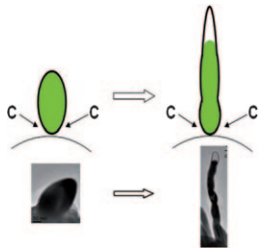

Fruity electrodes: A simple bottom-up self-assembly method was used to fabricate rambutan-like tin–carbon (Sn@C) nanoarchitecture (see scheme, green Sn) to improve the reversible storage of lithium in tin. The mechanism of the growth of the pear-like hairs is explored.

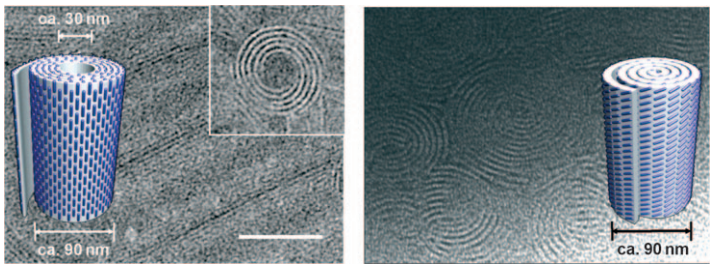

On a roll: Attachment of flexible coils to the middle of a rigid rod generates T-shaped rod–coil molecules that self-assemble into layers that roll up to form filled cylindrical and hollow tubular scrolls, depending on the coil length, in the solid state (see picture); the rods are arranged parallel to the layer plane.

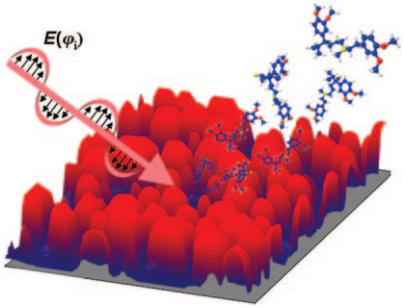

Nanoantennas for ions: Silicon microcolumn arrays harvest light from a laser pulse to produce ions. The system behaves like a quasi-periodic antenna array with ion yields that show profound dependence on the plane of polarization and the angle of incidence of the laser beam. Photonic ion sources promise to enable enhanced control of ion production on a micro- and nanometer scale and direct integration with miniaturized analytical devices.

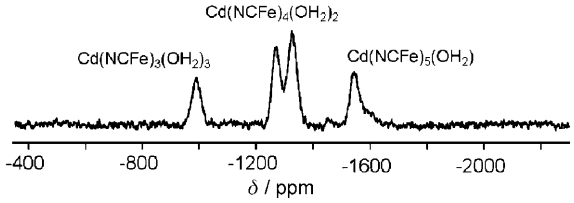

No legendary Prussian order! The distribution of vacancies in Prussian blue analogues is not random, and the spin density on the Cd^{2+} ion varies depending on the number of paramagnetic ions in its surroundings. This conclusion follows from ^{113}Cd solid-state magic-angle spinning NMR studies of $[Cd_3\{Fe/Co(CN)_6\}_2]\cdot 15\,H_2O$, where the presence of small but significant spin density on the observed ^{113}Cd nucleus leads to improved spectral resolution.

Contents

Service

Corrigendum

The authors have recently recognized an error in their Communication. A calculation error in the data of the energy density for HPGC materials in the organic electrolyte, as shown in Figure 3c, has been noticed but it does not influence their conclusions. The redrawn Figure 3c is plotted below. Correspondingly, the related statements on this topic (line 6–12, the first paragraph starting on page 375) should be corrected as following: "Even at a current drain time shorter than 2 s, the energy and power densities of HPGC were 10.8 Wh kg^{-1} and 21 kW kg^{-1}, respectively, thereby exceeding the PNGV power target; this result is comparable to that obtained for small-pore ECs at a drain time of about 6 s (that is, 23.8 Wh kg^{-11} and 15 kW kg^{-11}, calculated from the capacitance data given in Ref. [23])".
Additionally, the authors have given the power–energy density relation of HPGC material measured with ionic liquid ($BMImBF_4$) as a high-voltage electrolyte in the Figure 3c. The new result also confirms the promise and feasibility of HPGC materials for use in advanced supercapacitors with high power and energy densities.

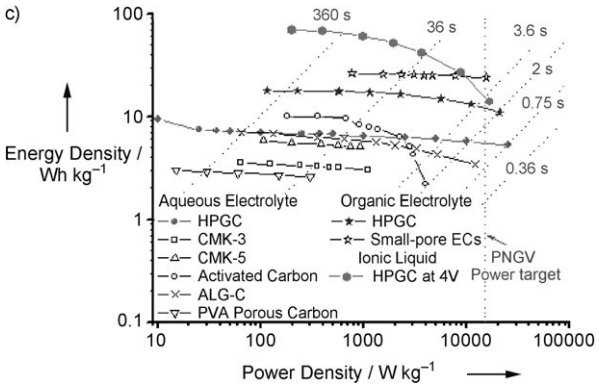

Figure 3. Electrochemical performance of the HPGC material: [...] c) Ragone plot showing the position of HPGC material relative to those of CMK-3, CMK-5,[19] activated carbon(Maxsorb, Japan), ALG-C,[16] PVA porous carbon,[22] and small-pore ECs.[23] The dotted lines show the current drain time. The weight of the cell components is not included in these *E*/*P* calculations. The compared *E*/*P* values were calculated from the capacitance data given in corresponding references. The PNGV power target (15 kW kg−1, in terms of electrode active material weight) is shown.

3D Aperiodic Hierarchical Porous Graphitic Carbon Material for High-Rate Electrochemical Capacitive Energy Storage

D.-W. Wang, F. Li, M. Liu, G. Q. Lu, H.-M. Cheng* — **373–376**

Angew. Chem. Int. Ed. **2008**, *47*

DOI 10.1002/anie.200702721

Corrigendum

Total Synthesis of Chondramide C and Its Binding Mode to F-Actin

H. Waldmann,* T.-S. Hu, S. Renner, S. Menninger, R. Tannert, T. Oda, H.-D. Arndt* _____ **6473–6477**

Angew. Chem. Int. Ed. **2008**, *47*

DOI 10.1002/anie.200801010

In this Communication, one image of the analysis of cellular phenotypes of chondramide C diastereoisomers was wrongly processed (panel C in Figure 1). An improved figure with additional scale bars can be found below. The authors deeply apologize for this oversight and confirm that it does not affect any of the hypothesis or conclusions outlined in the original paper.

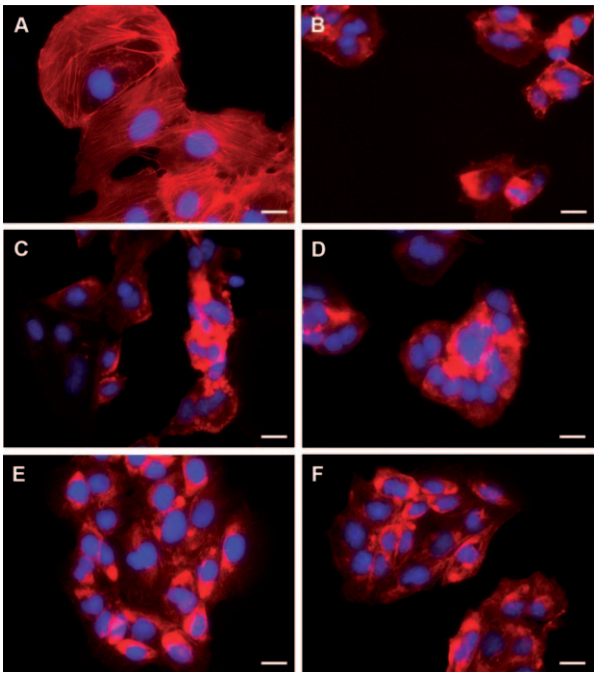

Figure 1. Actin stabilization phenotypes in BSC-1 cells monitored by whole cell fluorescence microscopy (magnification 40×) after staining for actin (red, TRITC-phalloidin, Sigma) and chromatin (blue, DAPI, Sigma); A) DMSO only (negative control); B) 100 nM Jasplakinolide (**2**, positive control); C) 10 μM *Z*/*E*-**14a**; D) 5 μM *Z*-**14b**; E) 200 nM *E*-**14c** (= **3**); F) 10 μM *E*-**14d**. TRITC: Tetramethylrhodamin isothiocyanate. Bar: 10 μm.

